

Original Article

Extended accelerated overrelaxation iteration techniques
in solving heat distribution problems

Khadeejah James Audu*

Department of Mathematics, Federal University of Technology, Minna, Nigeria

Received: 5 July 2021; Revised: 5 October 2021; Accepted: 24 August 2022

Abstract

Several stationary iteration techniques for numerical solutions to special systems of linear equation systems of the form $Au = b$ have been studied in an attempt to improve their convergence, suitability, and strength. Among such techniques is the Extended Accelerated Overrelaxation (EAOR) iterative scheme. In this paper, we studied the basics of the EAOR methods and applied them to compute the solution of a real-life problem, resolving the heat equation when a steady temperature is applied to a metal plate. We show how the real-life problem can be modeled into a partial differential equation, followed by discretization through the use of finite differences, and finally generating a largely sparse system of algebraic linear equations, from which the unknowns are to be solved. The techniques were compared with the Refinement of Accelerated Overrelaxation (RAOR) iterative scheme. The outcome of the numerical tests proves the effectiveness of the EAOR schemes for such problems.

Keywords: extended accelerated overrelaxation method, discretization, spectral radius, heat transfer, large linear equation system

1. Introduction

Many real world problems are usually represented in terms of mathematical concepts and equations, such as partial differential equations. These equations can be solved numerically through the use of discretization techniques. Among such techniques is the finite difference method. The finite difference procedure is a numerical analysis tool for providing approximate solutions to a wide range of scientific and engineering problems (Saad, 2003). The finite difference method works by dividing the area of interest into a certain number of mesh points and then giving each mesh point a unique identifier based on its location, like in heat transfer systems.

Some authors have come up with new, simple, and accurate ways to solve heat conduction problems in the past few years. These methods use meshless techniques. Heat conduction in nonlinear functionally graded materials can be simulated using a local semi-analytical meshless method, according to Wang, Wang, and Gong (2021). The method's

accuracy and validity have been demonstrated numerically through some case studies. Also, Chebyshev polynomials were used by Wang, Zhao, Chen, and Fan (2021) to develop a localized method for large-scale simulation of 2D boundary value problems. The method has great potential for solving elliptic partial differential equations quickly and accurately. Wang, Fan, Zheng, and Lin (2020) solved some problems with diffusion and convection-diffusion by using a localized space-time method of fundamental solutions. It is of utmost importance to utilize mathematics to fully understand and quantify any physical phenomenon. Such processes are usually transformed into systems of linear equations depicted as

$$Au = b \tag{1}$$

where, $A = [a_{ij}]$ is a non-singular ($\det A \neq 0$) square matrix. We split the matrix A into $A = D - A_L - A_U$ and impose the normalization to $D^{-1}A = D^{-1}b$ to get $A = \mathcal{L} - \mathcal{U}$, where $-\mathcal{L}$ and $-\mathcal{U}$ are strictly lower and upper triangular sections of A , and \mathcal{I} is the identity matrix.

Current stationary iteration techniques for computations of equation (1) by various researchers such as Assefa and Teklehaymanot (2021), Audu, Yahaya, Adeboye, and Abubakar (2021a), Tesfaye, Awgichew, Haile, and

*Corresponding author

Email address: k.james@futminna.edu.ng

Gashaye (2020); Vatti, Sri, and Mylapalli (2018); Vatti, Rao, and Pai (2020a); Wu and Yu-Jun (2014); and Youssef and Farid (2015) have been constructed to approximately find solutions to a square linear system of equations under special situations. Also, Vatti, Rao, and Pai (2020b) changed the Accelerated Overrelaxation approach and created the Reaccelerated Overrelaxation technique, which has a faster convergence rate than the Accelerated Overrelaxation technique. Some authors studied the performance of iteration methods for solutions to some systems of linear equations in case study applications. Authors like Akhir and Suleiman (2017) used a mix of triangle element approximation and an Accelerated Over-Relaxation approach to create an outstanding iterative technique for 2D Helmholtz equations. A numerical test was used to determine the method's performance. The linked Accelerated Over-Relaxation approach showed larger convergence improvements for the 2D Helmholtz equations than the Successive Over-Relaxation method, according to the results. Dahalan, Saudi, and Suleiman (2018) looked at how well the Quarter-sweep Accelerated Overrelaxation approach, which is a subset of the Accelerated Overrelaxation technique, solves robotic problems, such as finding a path from a starting point to a given destination in an indoor environment that doesn't have any collisions.

To numerically estimate the solution of the desired linear system in (1), we apply the EAOR technique presented by Audu, Yahaya, Adeboye, and Abubakar (2021a), described by

$$u^{(k+1)} = \mathcal{L}_{\beta,r,w}u^{(k)} + [\mathcal{J} - \beta\mathcal{L} - r\mathcal{A}]^{-1}w\bar{b} \quad (2)$$

where $\mathcal{L}_{\beta,r,w} = [\mathcal{J} - \beta\mathcal{L} - r\mathcal{A}]^{-1}[(1-w)\mathcal{J} + [w - \beta - r]\mathcal{L} + w\mathcal{U}]$ is the iteration matrix of the EAOR scheme. The parameters involved in the scheme represent overrelaxation, acceleration, and extended acceleration, respectively. The speed of convergence is assessed through the spectral radius, which is dependent on the iteration matrix. Usually, the convergence rate of a stationary iterative technique improves when the spectral radius is comparatively smaller. By setting certain options of the parameters in the EAOR technique (2), it reduces to the following well-known iteration techniques as special cases:

- Jacobi technique;
 $\mathcal{L}_{0,0,1} = [\mathcal{A}]^{-1}[\mathcal{L} + \mathcal{U}] + [\mathcal{A}]^{-1}\bar{b}$
- Gauss-Seidel technique;
 $\mathcal{L}_{0,1,1} = [\mathcal{J} - \mathcal{A}]^{-1}[\mathcal{U}] + [\mathcal{J} - \mathcal{A}]^{-1}\bar{b}$
- Successive Overrelaxation (SOR) technique;
 $\mathcal{L}_{0,w,w} = [\mathcal{J} - w\mathcal{A}]^{-1}[(1-w)\mathcal{J} + w\mathcal{U}] + w[\mathcal{J} - w\mathcal{A}]^{-1}\bar{b}$
- Accelerated Overrelaxation (AOR) technique;
 $\mathcal{L}_{0,r,w} = [\mathcal{J} - r\mathcal{A}]^{-1}[(1-w)\mathcal{J} + w\mathcal{U} + [w - r]\mathcal{L}] + w[\mathcal{J} - r\mathcal{A}]^{-1}\bar{b}$

In an endeavor to generalize the EAOR method to more classes of matrices, Audu, Yahaya, Adeboye, and Abubakar (2021b) extended the convergence domain of the EAOR technique to cover matrices. Despite the fact that the EAOR is a fast-converging technique compared to the AOR technique, it can attain faster convergence with more improvement. In light of this, Audu, Yahaya, Adeboye, and Abubakar (2021c) made the EAOR scheme even better so that it would converge faster. They proposed the refinement to

Extended Accelerated Overrelaxation (REAOR) technique:

$$\bar{u}^{(k+1)} = \left((\mathcal{J} - (\beta + r)\mathcal{L})^{-1}((1-w)\mathcal{J} + [w - (v + r)]\mathcal{L} + w\mathcal{U}) \right)^2 u^{(k)} + \left(\mathcal{J} + (\mathcal{J} - (\beta + r)\mathcal{L})^{-1}((1-w)\mathcal{J} + [w - (\beta + r)]\mathcal{L} + w\mathcal{U}) \right) (\mathcal{J} - (v + r)\mathcal{L})^{-1}w\bar{b} \quad (3)$$

The iteration matrix is given by $\left((\mathcal{J} - (\beta + r)\mathcal{L})^{-1}((1-w)\mathcal{J} + [w - (\beta + r)]\mathcal{L} + w\mathcal{U}) \right)^2$.

This current study is concerned with the application of the EAOR techniques to numerically estimate the solutions of sparse large linear systems, which are obtained when seeking the heat distribution in a metal plate that has different temperatures at its boundaries.

2. Steps for the EAOR Algorithm

1. Enter matrix \mathcal{A} , select an initial guess u^0 , maximum iteration number tolerance (ϵ) and $\beta, r, w \in (0,1)$
2. Obtain \mathcal{L}, \mathcal{U} and D from matrix \mathcal{A} and $D^{-1}\mathcal{A}$
3. Find the inverse of $[\mathcal{J} - \beta\mathcal{L} - r\mathcal{A}]$
4. Set $G = [\mathcal{J} - \beta\mathcal{L} - r\mathcal{A}]^{-1}[(1-w)\mathcal{J} + [w - \beta - r]\mathcal{L} + w\mathcal{U}]$
5. Set $V = w[\mathcal{J} - \beta\mathcal{L} - r\mathcal{A}]^{-1}\bar{b}$
6. Compute $u^{(k+1)} = Gu^{(k)} + V$
7. Stop if $\|u^{(k+1)} - u^{(k)}\|_{\infty} < \epsilon$

2.1. Steps for refinement EAOR algorithm

1. Enter matrix \mathcal{A} , select an initial guess u^0 , maximum iteration number tolerance (ϵ) and $\beta, r, w \in (0,1)$
2. Obtain \mathcal{L}, \mathcal{U} and D from matrix \mathcal{A} and $D^{-1}\mathcal{A}$
3. Find the inverse of $[\mathcal{J} - \beta\mathcal{L} - r\mathcal{A}]$
4. Set $T1 = (\mathcal{J} - (\beta + r)\mathcal{L})^{-1}((1-w)\mathcal{J} + [w - (\beta + r)]\mathcal{L} + w\mathcal{U})$
5. Set $T = \left((\mathcal{J} - (\beta + r)\mathcal{L})^{-1}((1-w)\mathcal{J} + [w - (\beta + r)]\mathcal{L} + w\mathcal{U}) \right)^2$
6. Set $P = (I + T1)(\mathcal{J} - (\beta + r)\mathcal{L})^{-1}(w\bar{b})$
7. Compute $u^{(k+1)} = Tu^{(k)} + P$
8. Stop if $\|\bar{u}^{(k+1)} - u^{(k)}\|_{\infty} < \epsilon$

3. Materials and Method

We consider a real-life problem, namely a two-dimensional heat distribution problem. This particular problem concerns a metal plate of size $0.9m \times 0.9m$ with the edges held at steady temperatures as in Figure 1 (Mayooran & Elliot, 2016).

3.1 Problem specification

Due to the fact that heat usually moves from a higher temperature to a lower temperature, for the metal plate given in Figure 1 we pose the problem of finding the temperature

distribution within the metal while in a steady state. What would the temperature be at each point?

3.2 Method of solution

We intend to find the temperatures within the metal plate in a stable state. For this, the metal plate is divided using a step-size along each axis, as displayed in Figure 2. After discretization of the plate, we get 64 inner grid nodes, which gives 64 unknowns. Each cell in the picture shows the temperature of a node of an element in the metal couple, with the edge of the metal plate in the middle of each node. It should be noted that the mesh points in Figure 2 are at the center of each element.

The aim is to examine the temperature distribution at each point in time. As it is typical with differential equations, it is easier to describe how this set-up changes from moment to moment. We write the physical dynamic model in the form of derivatives or partial derivatives, in what is known as the heat equation.

$$\frac{\partial T}{\partial t} - \alpha \left(\frac{\partial^2 T}{\partial x^2} + \frac{\partial^2 T}{\partial y^2} + \frac{\partial^2 T}{\partial z^2} \right) = 0 \tag{4}$$

The equation implies that as time increases, temperature changes over the three co-ordinates x , y and z . In this work, we consider only two dimensions y and x . Transforming the heat transfer problem into the Laplace equation:

$$\frac{\partial^2}{\partial x^2} T(x, y) + \frac{\partial^2}{\partial y^2} T(x, y) = 0 \tag{5}$$

for $0 \leq x \leq 0.9$ and $0 \leq y < 0.9$ combined with the following boundary conditions

$$\begin{aligned} T(x, 0) &= 273, & T(x, 0.9) &= 298, \\ T(0, y) &= 273 \text{ and } T(0.9, y) &= 373. \end{aligned} \tag{6}$$

Application of the central finite difference approximation to the partial derivatives $\frac{\partial^2 T}{\partial x^2}$ and $\frac{\partial^2 T}{\partial y^2}$ in (5) gives:

$$\frac{\partial^2 T}{\partial x^2} = \frac{T_{r+1,s} - 2T_{r,s} + T_{r-1,s}}{h^2} \tag{7}$$

$$\frac{\partial^2 T}{\partial y^2} = \frac{T_{r,s+1} - 2T_{r,s} + T_{r,s-1}}{k^2} \tag{8}$$

where (r, s) is the position on $x - y$ axes, with a discrete value range. Then, we have

$$\frac{T_{r+1,s} - 2T_{r,s} + T_{r-1,s}}{h^2} + \frac{T_{r,s+1} - 2T_{r,s} + T_{r,s-1}}{k^2} = 0 \tag{9}$$

For $k = h$, equation (9) becomes

$$4T_{r,s} - T_{r+1,s} - T_{r-1,s} - T_{r,s+1} - T_{r,s-1} = 0 \tag{10}$$

which signifies that, at each interior mesh-point, the temperature is the average of the temperatures of the four neighboring nodes of that specific mesh-point. Application of equation (9) to all the inner grid points generates a set of 64 algebraic linear equations:

$$\begin{aligned} 4t_{1,1} - t_{2,1} - t_{1,2} &= 546 \\ 4t_{2,1} - t_{3,1} - t_{1,1} - t_{2,2} &= 273 \\ 4t_{3,1} - t_{4,1} - t_{2,1} - t_{3,2} &= 273 \\ 4t_{4,1} - t_{5,1} - t_{3,1} - t_{4,2} &= 273 \\ 4t_{5,1} - t_{6,1} - t_{4,1} - t_{5,2} &= 273 \\ 4t_{6,1} - t_{7,1} - t_{5,1} - t_{6,2} &= 273 \\ 4t_{7,1} - t_{8,1} - t_{6,1} - t_{7,2} &= 273 \\ 4t_{8,1} - t_{7,1} - t_{8,2} &= 646 \\ 4u_{1,2} - t_{2,2} - t_{1,3} - t_{1,1} &= 273 \\ 4t_{2,2} - t_{3,2} - t_{1,2} - t_{2,3} - u_{2,1} &= 0 \\ 4t_{3,2} - t_{4,2} - t_{2,2} - t_{3,3} - t_{3,1} &= 0 \\ 4t_{4,2} - t_{5,2} - t_{3,2} - t_{4,3} - t_{4,1} &= 0 \\ 4t_{5,2} - t_{6,2} - t_{4,2} - t_{5,3} - t_{5,1} &= 0 \\ 4t_{6,2} - t_{7,2} - t_{5,2} - t_{6,3} - t_{6,1} &= 0 \\ 4t_{7,2} - t_{8,2} - t_{6,2} - t_{7,3} - t_{7,1} &= 0 \\ 4t_{8,2} - t_{7,2} - t_{8,3} - t_{8,1} &= 373 \\ 4t_{1,3} - t_{2,3} - t_{1,4} - t_{1,2} &= 273 \\ 4t_{2,3} - t_{3,3} - t_{1,3} - t_{2,4} - t_{2,2} &= 0 \\ 4t_{3,3} - t_{4,3} - t_{2,3} - t_{3,4} - t_{3,2} &= 0 \\ 4t_{4,3} - t_{5,3} - t_{3,3} - t_{4,4} - t_{4,2} &= 0 \\ 4t_{5,3} - t_{6,3} - t_{4,3} - t_{5,4} - t_{5,2} &= 0 \\ 4t_{6,3} - t_{7,3} - t_{5,3} - t_{6,4} - t_{6,2} &= 0 \\ 4t_{7,3} - t_{8,3} - t_{6,3} - t_{7,4} - t_{7,2} &= 0 \\ 4t_{8,3} - t_{7,3} - t_{8,4} - t_{8,2} &= 373 \\ 4t_{1,4} - t_{2,4} - t_{1,5} - t_{1,3} &= 273 \\ 4t_{2,4} - t_{3,4} - t_{1,4} - t_{2,5} - u_{2,3} &= 0 \\ 4t_{3,4} - t_{4,4} - t_{2,4} - t_{3,5} - t_{3,3} &= 0 \\ 4t_{4,4} - t_{5,4} - t_{3,4} - t_{4,5} - t_{4,3} &= 0 \\ 4t_{5,4} - t_{6,4} - t_{4,4} - t_{5,5} - t_{5,3} &= 0 \\ 4t_{6,4} - t_{7,4} - t_{5,4} - t_{6,5} - t_{6,3} &= 0 \\ 4t_{7,4} - t_{8,4} - t_{6,4} - t_{7,5} - t_{7,3} &= 0 \\ 4t_{8,4} - t_{7,4} - t_{8,5} - t_{8,3} &= 373 \\ 4t_{1,5} - t_{2,5} - t_{1,6} - t_{1,4} &= 273 \\ 4t_{2,5} - t_{3,5} - t_{1,5} - t_{2,6} - t_{2,4} &= 0 \\ 4t_{3,5} - t_{4,5} - t_{2,5} - t_{3,6} - t_{3,4} &= 0 \\ 4t_{4,5} - t_{5,5} - t_{3,5} - t_{4,6} - t_{4,4} &= 0 \\ 4t_{5,5} - t_{6,5} - t_{4,5} - t_{5,6} - t_{5,4} &= 0 \\ 4t_{6,5} - t_{7,5} - t_{5,5} - t_{6,6} - t_{6,4} &= 0 \\ 4t_{7,5} - t_{8,5} - t_{6,5} - t_{7,6} - t_{7,4} &= 0 \\ 4t_{8,5} - t_{7,5} - t_{8,6} - t_{8,4} &= 373 \\ 4t_{1,6} - t_{2,6} - t_{1,7} - t_{1,5} &= 273 \\ 4t_{2,6} - t_{3,6} - t_{1,6} - t_{2,7} - t_{2,5} &= 0 \\ 4t_{3,6} - t_{4,6} - t_{2,6} - t_{3,7} - t_{3,5} &= 0 \\ 4t_{4,6} - t_{5,6} - t_{3,6} - t_{4,7} - t_{4,5} &= 0 \\ 4t_{5,6} - t_{6,6} - t_{4,6} - t_{5,7} - t_{5,5} &= 0 \\ 4t_{6,6} - t_{7,6} - t_{5,6} - t_{6,7} - t_{6,5} &= 0 \\ 4t_{7,6} - t_{8,6} - t_{6,6} - t_{7,7} - t_{7,5} &= 0 \\ 4t_{8,6} - t_{7,6} - t_{8,7} - t_{8,5} &= 373 \end{aligned}$$

$$\begin{aligned}
 4t_{1,7} - t_{2,7} - t_{1,8} - t_{1,6} &= 273 \\
 4t_{2,7} - t_{3,7} - t_{1,7} - t_{2,8} - t_{2,6} &= 0 \\
 4t_{3,7} - t_{4,7} - t_{2,7} - t_{3,8} - t_{3,6} &= 0 \\
 4t_{4,7} - t_{5,7} - t_{3,7} - t_{4,8} - t_{4,6} &= 0 \\
 4t_{5,7} - t_{6,7} - t_{4,7} - t_{5,8} - t_{5,6} &= 0 \\
 4t_{6,7} - t_{7,7} - t_{5,7} - t_{6,8} - t_{6,6} &= 0 \\
 4t_{7,7} - t_{8,7} - t_{6,7} - t_{7,8} - t_{7,6} &= 0 \\
 4t_{8,7} - t_{7,7} - t_{8,8} - t_{8,6} &= 373 \\
 4t_{1,8} - t_{2,8} - t_{1,7} &= 571 \\
 4t_{2,8} - t_{3,8} - t_{1,8} - t_{2,7} &= 298 \\
 4t_{3,8} - t_{4,8} - t_{2,8} - t_{3,7} &= 298 \\
 4t_{4,8} - t_{5,8} - t_{3,8} - t_{4,7} &= 298 \\
 4t_{5,8} - t_{6,8} - t_{4,8} - t_{5,7} &= 298 \\
 4t_{6,8} - t_{7,8} - t_{5,8} - t_{6,7} &= 298 \\
 4t_{7,8} - t_{8,8} - t_{6,8} - t_{7,7} &= 298 \\
 4t_{8,8} - t_{7,8} - t_{8,7} &= 671
 \end{aligned} \tag{11}$$

The known boundary values of the plate are inserted into (11) to get a sparse and large 64×64 linear system $\mathcal{A}u = b$, which is represented as:

$$\begin{pmatrix}
 4 & -1 & 0 & 0 & 0 & 0 & 0 & 0 & -1 & 0 & 0 & \dots & 0 & 0 & 0 & 0 \\
 -1 & 4 & -1 & 0 & 0 & 0 & 0 & 0 & 0 & -1 & 0 & \dots & 0 & 0 & 0 & 0 \\
 0 & -1 & 4 & -1 & 0 & 0 & 0 & 0 & 0 & 0 & -1 & \dots & 0 & 0 & 0 & 0 \\
 0 & 0 & -1 & 4 & -1 & 0 & 0 & 0 & 0 & 0 & 0 & \dots & 0 & 0 & 0 & 0 \\
 0 & 0 & 0 & -1 & 4 & -1 & 0 & 0 & 0 & 0 & 0 & \dots & 0 & 0 & 0 & 0 \\
 0 & 0 & 0 & 0 & -1 & 4 & -1 & 0 & 0 & 0 & 0 & \dots & 0 & 0 & 0 & 0 \\
 0 & 0 & 0 & 0 & 0 & -1 & 4 & -1 & 0 & 0 & 0 & \dots & 0 & 0 & 0 & 0 \\
 0 & 0 & 0 & 0 & 0 & 0 & -1 & 4 & 0 & 0 & 0 & \dots & 0 & 0 & 0 & 0 \\
 -1 & 0 & 0 & 0 & 0 & 0 & 0 & 0 & 4 & -1 & 0 & \dots & 0 & 0 & 0 & 0 \\
 0 & -1 & 0 & 0 & 0 & 0 & 0 & 0 & -1 & 4 & -1 & \dots & 0 & 0 & 0 & 0 \\
 0 & 0 & -1 & 0 & 0 & 0 & 0 & 0 & 0 & -1 & 4 & \dots & 0 & 0 & 0 & 0 \\
 \vdots & \vdots & \vdots & \vdots & \vdots & \vdots & \vdots & \vdots & \vdots & \vdots & \vdots & \ddots & \vdots & \vdots & \vdots & \vdots \\
 0 & 0 & 0 & 0 & 0 & 0 & 0 & 0 & 0 & 0 & 0 & \dots & 4 & -1 & 0 & 0 \\
 0 & 0 & 0 & 0 & 0 & 0 & 0 & 0 & 0 & 0 & 0 & \dots & -1 & 4 & -1 & 0 \\
 0 & 0 & 0 & 0 & 0 & 0 & 0 & 0 & 0 & 0 & 0 & \dots & 0 & -1 & 4 & -1 \\
 0 & 0 & 0 & 0 & 0 & 0 & 0 & 0 & 0 & 0 & 0 & \dots & 0 & 0 & -1 & 4
 \end{pmatrix} \times \begin{pmatrix} t_{1,1} \\ t_{2,1} \\ t_{3,1} \\ t_{4,1} \\ t_{5,1} \\ t_{6,1} \\ t_{7,1} \\ t_{8,1} \\ t_{1,2} \\ t_{2,2} \\ t_{3,2} \\ \vdots \\ t_{5,8} \\ t_{6,8} \\ t_{7,8} \\ t_{8,8} \end{pmatrix} = \begin{pmatrix} 546 \\ 273 \\ 273 \\ 273 \\ 273 \\ 273 \\ 273 \\ 646 \\ 273 \\ 0 \\ 0 \\ \vdots \\ 298 \\ 298 \\ 298 \\ 671 \end{pmatrix} \tag{12}$$

where \mathcal{A} denotes the coefficient matrix of the linear equations, and b denotes the constant values at the right hand side, while u denotes the unknown variables. The linear system is then expressed as $\mathcal{D}^{-1}\mathcal{A}u = \mathcal{D}^{-1}b$ for the EAOR scheme in equation (3) to be applied in obtaining the 64 unknowns (u). Computations of spectral radius for different values of the EAOR parameters and comparison of the results with those of AOR technique were both carried out using Maple 2017 software package.

4. Results and Discussion

This section presents the numerical performance of the EAOR technique, in comparison with its refinement by Audu, Yahaya, Adeboye, and Abubakar (2021a) and the refinement of AOR by Vatti, Sri, and Mylapalli (2018), for the heat distribution problem analyzed in the previous section.

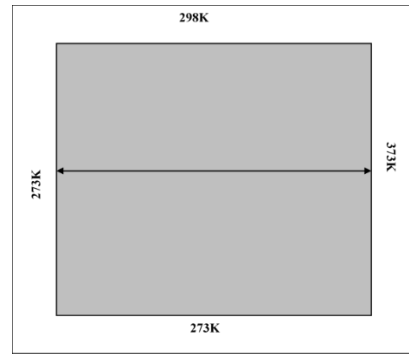


Figure 1. A metal plate with steady boundary conditions for temperature

298	298	298	298	298	298	298	298	298	298	298
273	$t_{1,8}$	$t_{2,8}$	$t_{3,8}$	$t_{4,8}$	$t_{5,8}$	$t_{6,8}$	$t_{7,8}$	$t_{8,8}$	373	373
273	$t_{1,7}$	$t_{2,7}$	$t_{3,7}$	$t_{4,7}$	$t_{5,7}$	$t_{6,7}$	$t_{7,7}$	$t_{8,7}$	373	373
273	$t_{1,6}$	$t_{2,6}$	$t_{3,6}$	$t_{4,6}$	$t_{5,6}$	$t_{6,6}$	$t_{7,6}$	$t_{8,6}$	373	373
273	$t_{1,5}$	$t_{2,5}$	$t_{3,5}$	$t_{4,5}$	$t_{5,5}$	$t_{6,5}$	$t_{7,5}$	$t_{8,5}$	373	373
273	$t_{1,4}$	$t_{2,4}$	$t_{3,4}$	$t_{4,4}$	$t_{5,4}$	$t_{6,4}$	$t_{7,4}$	$t_{8,4}$	373	373
273	$t_{1,3}$	$t_{2,3}$	$t_{3,3}$	$t_{4,3}$	$t_{5,3}$	$t_{6,3}$	$t_{7,3}$	$t_{8,3}$	373	373
273	$t_{1,2}$	$t_{2,2}$	$t_{3,2}$	$t_{4,2}$	$t_{5,2}$	$t_{6,2}$	$t_{7,2}$	$t_{8,2}$	373	373
273	$t_{1,1}$	$t_{2,1}$	$t_{3,1}$	$t_{4,1}$	$t_{5,1}$	$t_{6,1}$	$t_{7,1}$	$t_{8,1}$	373	373
273	273	273	273	273	273	273	273	273	273	273

Figure 2. Discretization of the plate with boundary conditions

Tables 1 and 2 show comparisons of the spectral radii and convergence results for the heat distribution problem, respectively. In Table 1, the notation for representing the iteration matrices of EAOR, refinement of EAOR and refinement of AOR is given as $\mathcal{L}_{\beta,r,w}$, $R\mathcal{L}_{\beta,r,w}$ and $R\mathcal{L}_{0,r,w}$ respectively. The designated matrix for EAOR iteration is $\mathcal{L}_{\beta,r,w} = [\mathcal{I} - \beta\mathcal{L} - r\mathcal{A}]^{-1}[w\mathcal{U} + (1-w)\mathcal{I} + [w - \beta - r]\mathcal{A}]$, for the refinement of EAOR it is $R\mathcal{L}_{\beta,r,w} = ((\mathcal{I} - (\beta + r)\mathcal{L})^{-1}((1-w)\mathcal{I} + [w - (\beta + r)]\mathcal{L} + w\mathcal{U}))^2$ and for refinement of AOR the matrix is $R\mathcal{L}_{0,r,w} = ((\mathcal{I} - (r)\mathcal{L})^{-1}((1-w)\mathcal{I} + [w - r]\mathcal{L} + w\mathcal{U}))^2$. The Extended AOR, its refinement, and AOR refinement techniques in terms of their spectral radii for the heat distribution problem, with different values of r , β and w are shown in Table 1. It is observed that the spectral radii of $\mathcal{L}_{r,w}$, $R\mathcal{L}_{\beta,r,w}$ and $R\mathcal{L}_{0,r,w}$ are smaller than 1. However, on observation of how close their spectral radii are to zero, it is concluded that the rate of convergence of the refinement of the EAOR technique is more rapid than that of the EAOR and refinement AOR techniques due to the fact that $\rho(\mathcal{L}_{\beta,r,w}) < \rho R(\mathcal{L}_{0,r,w}) < \rho R(\mathcal{L}_{\beta,r,w}) < 1$. Figure 4 shows the comparison of the three iteration techniques for clarity. This indicates that refined EAOR will converge to the true solution more rapidly than the compared methods.

298	298	298	298	298	298	298	298	298	298	298
273	286.49	292.57	296.35	299.65	303.43	308.66	317.16	333.69	373	373
273	282.39	289.43	295.19	300.84	307.40	316.03	328.31	346.58	373	373
273	280.63	287.56	294.14	301.10	309.32	319.75	333.47	351.33	373	373
273	279.57	286.05	292.71	300.12	309.01	320.19	334.47	352.30	373	373
273	278.60	284.34	290.53	297.67	306.40	317.53	331.92	350.36	373	373
273	277.49	282.20	287.42	293.61	301.40	311.61	325.34	344.23	373	373
273	276.16	279.52	283.33	287.96	293.97	302.17	313.58	328.23	373	373
273	274.64	276.39	278.41	280.93	284.36	289.53	298.58	318.20	373	373
273	273	273	273	273	273	273	273	273	273	273

Figure 3. The solved distribution of temperature

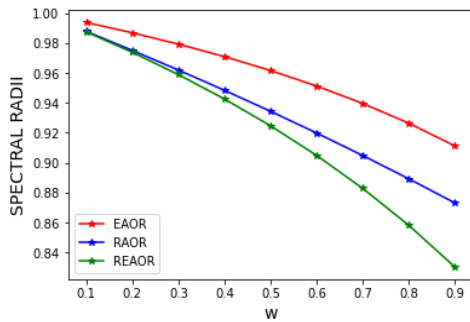


Figure 4. Spectral radii of iteration matrices for EAOR, RAOR and REAOR

Table 2 displays the convergence results for the heat transfer problem. It is seen that the refined Extended Accelerated Overrelaxation technique has a lesser number of iterations and takes a shorter time to solve the linear system to an accuracy of 10^{-10} in comparison with the refined Accelerated Overrelaxation technique and Extended Accelerated Overrelaxation technique. This proves that the convergence speed of the refined EAOR technique for the heat distribution problem is faster than the performance of the EAOR techniques and refined AOR technique. The values of

$$u = \begin{bmatrix} 274.64, 276.39, 278.41, 280.93, 284.36, 289.53, 298.58, 318.20, 276.16, 279.52, 283.33, \\ 153287.96, 293.97, 302.17, 313.58, 328.23, 277.49, 282.20, 287.42, 293.61, 301.40, 311.61, \\ 325.34, 154344.23, 278.60, 284.34, 290.53, 297.67, 306.40, 317.53, 331.92, 350.36, 279.57, \\ 286.05, 292.71, 155300.12, 309.01, 320.19, 334.47, 352.30, 280.63, 287.56, 294.14, 301.10, \\ 309.32, 319.75, 333.47, 156351.33, 282.39, 289.43, 295.19, 300.84, 307.40, 316.03, 328.31, \\ 346.58, 286.49, 292.57, 296.35, 157299.65, 303.43, 308.66, 317.16, 333.69 \end{bmatrix} \quad (13)$$

Table 1. Comparison of EAOR, Refined AOR and Refined EAOR for spectral radii of their iteration matrices

w	β	r	$\rho(\varphi_{\beta,r,w})$	$\rho R(\varphi_{0,r,w})$	$\rho R(\varphi_{\beta,r,w})$
0.1	0.04	0.05	0.9936764826	0.9876928421	0.9873929521
0.2	0.08	0.10	0.9867694121	0.9749874636	0.9737138726
0.3	0.12	0.15	0.9791905790	0.9618640645	0.9588141901
0.4	0.16	0.20	0.9708322197	0.9483015040	0.9425151988
0.5	0.20	0.25	0.9615610144	0.9342771858	0.9245995844
0.6	0.24	0.30	0.9512096225	0.9197669305	0.9047997459
0.7	0.28	0.35	0.9395644282	0.9047448361	0.8827813147
0.8	0.32	0.40	0.9263472516	0.8891831220	0.8581192305
0.9	0.36	0.45	0.9111870362	0.8730519581	0.8302618150

the unknowns (u) are obtained as in equation (13) and substituted into Figure 2 to obtain Figure 3.

Table 2. Convergence results for the heat transfer problem

Iterative technique	Number of iterations	CPU time (seconds)
Refined AOR	226	0.500
EAOR	300	0.531
Refined EAOR	152	0.400

5. Conclusions

This paper has demonstrated the significance of the Extended Accelerated Over-relaxation techniques for accelerating solutions of systems of algebraic linear equations that stem from real-life problems, such as the heat distribution problem considered in the study. Due to its speed and ability to solve large linear systems, the refinement EAOR can be considered an appropriate technique when solving sparse and large linear systems. Further study can consider finding optimum values of the three parameters to attain rapid convergence and comparing the EAOR techniques with non-stationary iteration techniques like the conjugate gradient method for speedy convergence.

References

Akhir, M., K., M. & Suleiman, J. (2017). Accelerated Over-Relaxation iterative method using triangle element approximation for solving 2D helmhotz equations. *Journal of Physics, Conference Series*, 890(1), 1-5. doi:10.1088/1742-6596/890/1/012060.

Assefa, L. W., & Teklehaymanot, A. W. (2021). Second refinement of accelerated over relaxation method for the solution of linear system. *Pure and Applied Mathematics Journal*, 10(1), 32-37. doi:10.11648/j.pamj.20211001.13.

- Audu, K. J., Yahaya, Y. A., Adeboye, K. R., & Abubakar, U. Y. (2021a). Extended accelerated over relaxation (EAOR) method for solution of a large and sparse linear system. *Journal of Science, Technology, Mathematics and Education*, 17(1), 228-236.
- Audu, K. J., Yahaya, Y. A., Adeboye, K. R., & Abubakar, U. Y. (2021b). Refinement of extended accelerated over relaxation method for solution of linear systems. *Nigerian Annals of Pure and Applied Sciences*, 4(1), 51-61. doi:10.46912/napas.226.
- Audu, K. J., Yahaya, Y. A., Adeboye, K. R. & Abubakar, U. Y. (2021c). Convergence of triple accelerated over relaxation (TAOR) for M-matrix linear systems. *Iranian Journal of Optimization*, 13(2)
- Dahalan, A. A., Saudi, A. M. & Suleiman, H. (2018). Numerical technique for autonomous robot path planning based on QSAOR iterative method using indoor environment. *Journal of Engineering and Applied Sciences*. 13(20), 8414-8418. doi:10.36478/jeasci.2018.8414-8418.
- Mayooran, T., & Elliot, L. (2016). Applying the successive over-relaxation method to a real world problems. *American Journal of Applied Mathematics and Statistics*, 4(4), 113-117. doi:10.12691/ajams-4-4-3.
- Saad, Y. (2003). *Iterative methods for sparse linear systems*. Philadelphia, PA: Society for Industrial and Applied Mathematics. doi:10.1137/1.9780898718003.
- Tesfaye, K. E., Awgichew, G., Haile, E., & Gashaye, D. A. (2020). Second refinement of Gauss-Seidel iteration method for solving linear system of equations. *Ethiopia Journal of Science and technology*, 13(1), 1-15. doi:10.4314/ejst.v13i1.1.
- Vatti, K., Sri, R., & Mylapalli, M. S. (2018). A refinement of accelerated over relaxation method for the solution of linear systems. *International Journal of Pure and Applied Mathematics*, 118(18), 1571-1577.
- Vatti, V. B. K., Rao, G. C., & Pai, S. S. (2020a). Parametric Accelerated Over relaxation (PAOR) method. *Numerical Optimization in Engineering and Sciences, Advances in Intelligent Systems and Computing*, 979, 283-288. doi:10.1007/978-981-15-3215-3_27
- Vatti, V. B. K., Rao, G., C. & Pai, S. S. (2020). Reaccelerated over-relaxation (ROR) method. *Bulletin of the International Mathematical Virtual Institute*, 10(2), 315-324. doi:10.7251/BIMVI2002315K.
- Wang, C., Wang, F. & Gong, Y. (2021). An analysis of 2D heat conduction in nonlinear functionally graded materials using a local semi-analytical meshless method. *AIMS Mathematics*, 6(11), 12599-12618. doi:10.3934/math.2021726.
- Wang, F., Fan, C., Zhang, C. & Lin, J. (2020). A localized spaced-time method of fundamental solutions for diffusion and convection-diffusion problems. *Advance Applied Mathematics and Mechanics*, 12(4), 940-958. doi:10.4208/aamm.OA-2019-0269.
- Wang, F., Zhao, Q., Chen, Z. & Fan, C. (2020). Localized chebyshev collocation method for solving elliptic partial differential equations in arbitrary 2D domains. *Applied Mathematics and Computations*, 397. doi:10.1016/j.amc.2020.125903.
- Wu, S., & Yu-Jun, L. (2014). A new version of accelerated over-relaxation iterative method. *Journal of Applied Mathematics*, 2014, 1-6. doi:10.1155/2014/725360.
- Youssef, I. K., & Farid, M. M. (2015). On the accelerated over-relaxation method. *Pure and Applied Mathematics*, 4(1), 26-31. doi:10.11648/j.pamj.20150401.14.